



Published in final edited form as:

Gastroenterology. 2015 December ; 149(7): 1932–1943.e9. doi:10.1053/j.gastro.2015.07.058.

STAT3 Mediated Remodeling of the Tumor Microenvironment Results in Enhanced Tumor Drug Delivery in a Mouse Model of Pancreatic Cancer

Nagaraj S. Nagathihalli^{1,*}, Jason A. Castellanos^{2,*}, Chanjuan Shi³, Yugandhar Beesetty², Michelle L. Reyzer⁴, Richard Caprioli⁴, Xi Chen⁵, Alex J. Walsh⁶, Melissa C. Skala⁶, Harold L. Moses⁷, and Nipun B. Merchant¹

¹Division of Surgical Oncology, Department of Surgery, University of Miami Miller School of Medicine, Sylvester Comprehensive Cancer Center, Miami, Florida

²Department of Surgery, Vanderbilt University School of Medicine, Nashville, Tennessee

³Department of Pathology, Vanderbilt University School of Medicine, Nashville, Tennessee

⁴Department of Biochemistry, Vanderbilt University School of Medicine, Nashville, Tennessee

⁵Department of Biostatistics, Vanderbilt University School of Medicine, Nashville, Tennessee

⁶Department of Biomedical Engineering, Vanderbilt University School of Medicine, Nashville, Tennessee

⁷Department of Cancer Biology, Vanderbilt University School of Medicine, Nashville, Tennessee

Corresponding Author: Nipun B. Merchant, Division of Surgical Oncology, University of Miami Miller School of Medicine, 1120 NW 14th Street, CRB 410, Miami, Florida 33136 Phone: 305-243-9517 nmerchant@miami.edu.

*Nagaraj S. Nagathihalli and Jason A. Castellanos contributed equally to this work.

Publisher's Disclaimer: This is a PDF file of an unedited manuscript that has been accepted for publication. As a service to our customers we are providing this early version of the manuscript. The manuscript will undergo copyediting, typesetting, and review of the resulting proof before it is published in its final citable form. Please note that during the production process errors may be discovered which could affect the content, and all legal disclaimers that apply to the journal pertain.

Conflict of Interest: The authors declare no conflicts of interest.

Author Contributions:

Nagaraj Nagathihalli – study concept and design; acquisition of data; analysis and interpretation of data; drafting of the manuscript; critical revision of the manuscript for important intellectual content; study supervision

Jason Castellanos – study concept and design; acquisition of data; analysis and interpretation of data; drafting of the manuscript; critical revision of the manuscript for important intellectual content; statistical analysis

Chanjuan Shi – analysis and interpretation of data; critical revision of the manuscript for important intellectual content; technical support

Yugandhar Beesetty – acquisition of data

Michelle Reyzer – study concept and design; acquisition of data; analysis and interpretation of data; critical revision of the manuscript for important intellectual content

Richard Caprioli – study concept and design; critical revision of the manuscript for important intellectual content; material support; study supervision

Xi Chen – study concept and design; statistical analysis

Alex Walsh – study concept and design; acquisition of data; analysis and interpretation of data; critical revision of the manuscript for important intellectual content; statistical analysis

Melissa Skala – study concept and design; acquisition of data; analysis and interpretation of data; critical revision of the manuscript for important intellectual content; study supervision

Harold Moses – study concept and design; critical revision of the manuscript for important intellectual content; material support

Nipun Merchant – study concept and design; analysis and interpretation of data; critical revision of the manuscript for important intellectual content; obtained funding; material support; study supervision

Abstract

BACKGROUND & AIMS—A hallmark of pancreatic ductal adenocarcinoma (PDAC) is the presence of a dense desmoplastic reaction (stroma) that impedes drug delivery to the tumor. Attempts to deplete the tumor stroma have resulted in formation of more aggressive tumors. We have identified STAT3 as a biomarker of resistance to cytotoxic and molecularly targeted therapy in PDAC. The purpose of this study is to investigate the effects of targeting STAT3 on the PDAC stroma and on therapeutic resistance.

METHODS—Activated STAT3 protein expression was determined in human pancreatic tissues and tumor cell lines. *In vivo* effects of AZD1480, a JAK/STAT3 inhibitor, gemcitabine or the combination were determined in *Ptfl1^{cre/+};LSL-Kras^{G12D/+};Tgfr2^{flx/flx}* (PKT) mice and in orthotopic tumor xenografts. Drug delivery was analyzed by MALDI-imaging mass spectrometry. Collagen second harmonic generation (SHG) imaging quantified tumor collagen alignment and density.

RESULTS—STAT3 activation correlates with decreased survival and advanced tumor stage in patients with PDAC. STAT3 inhibition combined with gemcitabine significantly inhibits tumor growth in both an orthotopic and the PKT mouse model of PDAC. This combined therapy attenuates *in vivo* expression of SPARC, increases microvessel density and enhances drug delivery to the tumor without depletion of stromal collagen or hyaluronan. Instead, the PDAC tumors demonstrate vascular normalization, remodeling of the tumor stroma and downregulation of cytidine deaminase (Cda).

CONCLUSIONS—Targeted inhibition of STAT3 combined with gemcitabine enhances *in vivo* drug delivery and therapeutic response in PDAC. These effects occur through tumor stromal remodeling and downregulation of Cda without depletion of tumor stromal content.

Keywords

drug delivery; tumor microenvironment; stroma; pancreatic cancer

Introduction

Pancreatic ductal adenocarcinoma (PDAC) remains a major therapeutic challenge. The five-year survival is approximately 5% and has not changed significantly over the past 40 years.¹ The poor response of PDAC patients to targeted and systemic therapies may be due to impedance of drug delivery to the tumor by its dense desmoplastic stroma, a hallmark of both mouse and human PDAC.^{2, 3} This marked fibrosis (desmoplasia) is characterized by a poorly functioning vasculature that has variable blood flow through leaky, immature vessels, resulting in increased interstitial fluid pressure.^{4, 5} Targeted inhibition of the Hedgehog pathway has been shown to deplete the tumor stroma, resulting in a transient increase in intratumoral perfusion, enhanced delivery of gemcitabine to the tumor and stabilization of disease in a mouse model of PDAC.⁶ Recent studies, however, have demonstrated that tumor stroma may also play an important role in restraining PDAC.^{7, 8} Therefore, therapeutic efficacy and improved survival hinge on treatments that enhance drug delivery without incurring the negative consequences of stromal depletion.

Pancreatic stellate cells (PSC) and myeloid derived suppressor cells (MDSC) in the PDAC tumor microenvironment (TME) produce factors to create a pro-tumorigenic environment. Within the TME, PSCs are known to secrete several factors, including IL-6, which can activate JAK-mediated STAT3 signaling and induce stromally mediated local immunosuppression through the expansion of MDSCs.⁹ We have recently demonstrated a mechanistic rationale for activated STAT3 as a biomarker of therapeutic resistance in PDAC.¹⁰ Targeted inhibition of STAT3 may therefore directly impact the TME to improve therapeutic response.

Genetically engineered mouse models (GEM) of PDAC progression are invaluable tools to study tumor stromal interactions.¹¹ Ijichi, et al. developed the *Ptfla^{cre/+};LSL-Kras^{G12D/+};Tgfb²^{flox/flox}* (PKT) GEM of PDAC which develops autochthonous well-differentiated PDAC with abundant stroma. Of the PDAC GEMs, the PKT mouse represents the closest stromal approximation to human PDAC.^{12–14} Additionally, this model displays constituent STAT3 activation in both the epithelial and stromal components of the TME.¹⁵ Therefore, the PKT GEM provides a clinically and molecularly relevant tool to probe the role of STAT3 in the PDAC TME.

In this study, we demonstrate that STAT3 activation increases with the step-wise progression from precancerous lesions to PDAC in human and mouse tumors. PDAC patients with tumors that have high levels of activated STAT3 expression exhibit higher tumor grades, more advanced stages of disease, and decreased overall survival (OS). To target JAK-mediated activation of STAT3 we used AZD1480, a JAK-selective small molecule inhibitor. STAT3 inhibition combined with gemcitabine results in significantly increased tumor microvessel density, enhanced *in vivo* drug delivery and improved survival in both xenograft mouse models and PKT mice. These effects are seen without depletion of collagen or hyaluronan content within the tumor, but rather through remodeling of the tumor stroma and downregulation of cytidine deaminase (Cda) within PDAC tumors. Taken together, these results suggest that combining STAT3 inhibition with gemcitabine is a promising therapeutic strategy for PDAC.

Results

Total and Activated STAT3 Expression in Human Pancreas Tissues and Cell Lines

A tissue microarray (TMA) of patient samples was examined for total and activated STAT3 (pSTAT3) expression in order to determine the expression of STAT3 in normal pancreatic and PDAC tissue. Analysis confirmed a step-wise increase of both total (Figure 1A) and pSTAT3 expression (Figure 1B) from normal pancreas to chronic pancreatitis through advancing grade and stage of PDAC, indicating that STAT3 expression and activation increases with the progression of pancreatic neoplasia. Furthermore, patients with PDAC tumors that expressed high levels of pSTAT3 had significantly higher tumor grade, stage, and lower OS when compared to patients with tumors that had low pSTAT3 expression (median survival of 14 months vs 22 months respectively, $p = 0.029$, Figure 1C, Supplemental Table 1).

The expression levels of total and pSTAT3 were characterized in nine human PDAC cell lines, a pancreatic intraepithelial neoplasia (PanIN) cell line derived from the *LSL-Kras^{G12D/+}; Pdx1^{Cre/+}* (KC) GEM, and primary PDAC (PDA) and liver metastasis (LMP) cell lines derived from the *LSL-Kras^{G12D/+}; Trp53^{R172H/+}; Pdx1^{Cre/+}* (KPC) GEM.^{16, 17} We have previously characterized the sensitivity of these nine human PDAC cell lines to various therapeutic agents including AZD1480 (Supplemental Table 2).¹⁸ The resistant human cell lines (PANC1, MiaPaCa2 and CFPAC) as well as the murine metastatic cell line (LMP), were found to have the highest baseline expression of pSTAT3, while the highly sensitive human cell lines (BxPC3, HPAC) and mouse PanIN cells had little or no baseline expression of pSTAT3 (Figure 1D). Expression of other isoforms of STAT, such as STAT5, did not show variable expression in these cell lines (data not shown).

Pharmacologic JAK-STAT3 inhibition with AZD1480 revealed a dose- and time-dependent down regulation of pSTAT3 levels in the resistant PANC1 and MiaPaCa2 cell lines (Supplemental Figure 1A and B). Stattic, a small molecule that specifically inhibits the SH2 domain of STAT3, also significantly decreased pSTAT3 levels in the resistant MiaPaCa2 and LMP cell lines (Supplemental Figure 1C).¹⁹ Knockdown of STAT3 in PANC1 cells (sh-STAT3 PANC1) also resulted in significantly decreased colony formation (Supplemental Figure 2A).

STAT3 Inhibition Combined with Gemcitabine Effectively Inhibits PDAC Tumor Growth *In Vivo*

We next sought to determine the efficacy of STAT3 inhibition *in vivo*. Mice were inoculated subcutaneously (s.c., n = 5/group) with PANC1 cells. Tumor bearing mice were treated with AZD1480 and gemcitabine either individually or in combination. Compared with vehicle treated mice, tumor volume was significantly decreased in mice treated with AZD1480 (p < 0.001) or gemcitabine alone (p < 0.001). The combination of AZD1480 and gemcitabine, however, resulted in the optimal treatment effect and tumor regression and was superior to both vehicle and monotherapy (p < 0.001, Figure 2A). The combination therapy was well tolerated and did not result in any significant *in vivo* toxicity (Supplemental Figure 3A).

Orthotopic tumors were induced with direct pancreatic injections of luciferase-tagged PANC1 cells, and bioluminescence imaging (BLI) was utilized to monitor orthotopic tumor growth and treatment response. Tumor-bearing mice treated with the same regimens as above underwent BLI prior to initiation of treatment and then weekly thereafter. There was a trend towards the mean photon emission over the treatment interval being lowest in the groups that received either AZD1480 or the combination of AZD1480 and gemcitabine but this did not achieve statistical significance (Supplemental Figure 4). This decline in signal correlated with decreased tumor growth (data not shown). Immunoblotting of orthotopic xenograft tumor lysates demonstrated significant inhibition of STAT3 phosphorylation (Figure 2B).

STAT3 Inhibition Combined with Gemcitabine Alters the PDAC TME

To determine the mechanism responsible for the synergistic antitumor activity of JAK-STAT3 inhibition and gemcitabine treatment, we focused on stromal effectors of STAT3

activation. STAT3-specific inhibition with Stattic resulted in decreased SPARC expression levels in the resistant MiaPaCa2 and PANC1 cell lines (Supplemental Figure 1D). Orthotopic and flank tumors treated with AZD1480 or AZD1480 and gemcitabine had significantly decreased pSTAT3 and epithelial SPARC expression (Figure 2B and 2C and Supplemental Figure 5A). Immunoblotting of STAT3 sh-RNA PANC1 flank xenografts confirmed that these findings were specifically related to STAT3 inhibition and not an off treatment effect of AZD1480 (Figure 2D).

Combined treatment with AZD1480 and gemcitabine also resulted in significantly increased CD31+ staining and microvessel density in both orthotopic and flank tumor xenografts when compared with vehicle control and monotherapy treated tumors (Figure 2E, Supplemental Figure 5B). Therefore, this combined therapy alters stromal composition by attenuating the expression of SPARC and increasing microvessel density within the TME.

STAT3 Inhibition Combined with Gemcitabine Inhibits Tumor Growth and Improves Survival in PKT Mice

To further explore the effect of STAT3 inhibition on the tumor stroma, we utilized the PKT mouse model. These mice develop autochthonous PDAC with full penetrance that reliably recapitulates the clinical and histopathological features of the human disease. They consistently develop PanIN lesions at 3.5 weeks of age and progress to invasive cancer by 4.5 weeks of age. Median overall survival of PKT mice is consistently around 59 days.¹² Treatments were initiated at 4 weeks of age and mice were allowed to progress with PDAC until they died or became moribund. Tumor weight was significantly reduced in mice treated with AZD1480 and gemcitabine compared with vehicle treated mice (Figure 3A), without significant additive toxicity (as indicated by change in mouse body weight, Supplemental Figure 3B). Immunoblot analyses of whole-tumor lysates showed decreased expression of pSTAT3 and SPARC with either AZD1480 or combined AZD1480 and gemcitabine treatment (Figure 3B). CD31 staining and microvessel density were also significantly enhanced in mice treated with the combination therapy (Figure 3C). PKT mice treated with either AZD1480 or gemcitabine alone showed no survival benefit compared with vehicle treated mice (Supplemental Figure 6). In contrast, treatment with AZD1480 and gemcitabine significantly extended the median survival of PKT mice (52 vs. 60 days, $p = 0.033$, log-rank test) (Figure 3D).

Treatment with AZD1480 and Gemcitabine Results in Significantly Enhanced *In Vivo* Drug Delivery

Matrix-assisted laser desorption/ionization (MALDI) imaging mass spectrometry (IMS), an excellent tool for visualizing small molecules in tissue sections,^{20, 21} was utilized to determine the presence and localization of AZD1480 and gemcitabine (Supplemental Figure 7A and B) in subcutaneous (Figure 4A) and orthotopic (Figure 4B) xenograft tumors. While AZD1480 was present in tumors of mice treated with AZD1480 monotherapy, there was no evidence of gemcitabine penetrance in the tumors of mice treated with gemcitabine alone. Mice treated with AZD1480 and gemcitabine demonstrated significantly enhanced tumor penetrance of both AZD1480 and gemcitabine to the tumor (Supplemental Figure 8A and

B). These results show that *in vivo* tumor drug delivery is significantly enhanced with combined AZD1480 and gemcitabine treatment.

Increased Tumor Drug Delivery is Not Due to Depletion of the Tumor Stroma

We next sought to determine whether the enhanced antitumor effect and drug delivery with AZD1480 and gemcitabine treatment was due to depletion of the tumor stroma. In addition to collagen, hyaluronan is an important constituent of the stroma and has been implicated as a potential barrier to drug delivery in PDAC.²² IHC quantification of hyaluronan and collagen in tissues stained for hyaluronan binding protein, collagen IV and trichrome blue, respectively (Figure 5*A* and *B*) demonstrated no significant changes in stromal content between treatment groups. Analysis of H&E and α Smooth Muscle Actin stained slides failed to demonstrate any difference in the inflammatory cell infiltrate or myofibroblast composition of the tumor stroma of untreated vs. treated tumors (data not shown). Furthermore, there was no difference in the collagen content of STAT3-shRNA PANC1 tumor xenografts when compared with sh-scrambled control PANC1 tumors (Figure 5*C*).

Magnetization Transfer (MT)-MRI imaging provides a correlation of the level of fibrosis within tissues.²³ No significant difference in the longitudinal assessment of magnetization transfer ratio (MTR) signal between vehicle versus monotherapy or the combination treatment in PKT mice was seen despite a slower rate of tumor growth (Figure 5*D*, *E* and *F*). Contrary to our expectations, treatment with AZD1480 and gemcitabine did not deplete collagen or hyaluronan content despite the decrease in tumor size, decreased expression of the stromal effector SPARC and enhanced drug delivery to the tumor.

Improved Therapeutic Response is Mediated by Stromal Remodeling and Downregulation of Cytidine Deaminase

To further define the effect of AZD1480 and gemcitabine treatment on the tumor stroma, second harmonic generation (SHG) images of PKT mouse tumors were obtained and analyzed (Figure 6*A*). Multiphoton SHG imaging allows specific imaging of collagen fibers as well as analysis of fiber orientation and quantification within tissue samples, making it a potent tool to investigate collagen organization, quantity, and remodeling.²⁴ Analysis of collagen density revealed no difference between treatment groups, further confirming the lack of collagen depletion. However, the coefficient of collagen fiber alignment was significantly decreased and the angle variance was significantly increased with the combination therapy, indicating less parallel fiber alignment and increased variation in fiber direction, respectively. This data indicates that treatment with AZD1480 and gemcitabine results in tumor stroma that has significantly fewer parallel collagen fibers than vehicle or monotherapy treated tumors. Analysis of the angle distribution showed that the tumors treated with the combined therapy also had significantly lower kurtosis, indicating a less skewed distribution of collagen fiber rearrangement. Thus, treatment with AZD1480 and gemcitabine results in significant stromal remodeling with greater collagen fiber disorganization, rather than collagen depletion, while still significantly decreasing tumor size.

Gemcitabine can be enzymatically inactivated by Cda, which is highly expressed in murine PDA neoplastic cells.²⁵ Due to the enhanced delivery of gemcitabine when combined with AZD1480, we analyzed PKT mouse tumor lysates for Cda expression. There was significant downregulation of Cda levels with AZD1480 treatment as well as combined AZD1480 and gemcitabine treatment (Figure 6B). Monotherapy with gemcitabine actually led to increased tumor Cda expression. Immunoblotting of Cda in STAT3 sh-RNA PANC1 cells confirmed that the change in Cda expression is specifically related to STAT3 inhibition and not off-target effects of AZD1480 (Supplemental Figure 9). These findings are consistent with the lack of drug delivery seen on MALDI-IMS of gemcitabine treated tumors. These results show that the treatment effect of AZD1480 combined with gemcitabine results in remodeling of the tumor stroma without depletion of collagen content and downregulation of Cda expression, leading to enhanced drug delivery to the tumor (Figure 6C and D).

Discussion

The focus of this study was to study the effect of STAT3 inhibition on the tumor stroma in PDAC. Our previous work has provided compelling evidence establishing STAT3 as a key mediator of chemoresistance in PDAC.^{10, 18} Further confirming these results, we now show a clear association between pSTAT3 expression levels in patient PDAC tumors and poor prognosis. Interestingly, total STAT3 expression also rises with advancing grades of tumor. Recent studies have demonstrated that non-phosphorylated STAT3 may translocate to the nucleus and stimulate expression of pro-inflammatory genes in a distinct manner from pSTAT3.^{26, 27} Activated STAT3 signaling in tumor cells acts as a crucial oncogenic mediator and is critical to the interplay between stromal and pre-neoplastic pancreatic cells.²⁸ Taken together, these findings provide strong evidence that disrupting STAT3 signaling blocks a key interface of tumor-stromal interaction in PDAC.

Targeting JAK/STAT3 exerts a significant antitumor effect *in vivo* and has a direct impact on the TME. Our findings indicate that STAT3 inhibition consistently downregulates SPARC expression, and when combined with gemcitabine leads to a significant increase in microvessel density of the tumor. Pancreatic cancer is notable for its dysfunctional vasculature and hypoxic TME, and while anti-angiogenic targeted therapy has been ineffective in clinical trials, the ability to induce vascular normalization may result in significantly improved clinical outcomes through increased drug delivery and anti-tumor effects.²⁹

Recent findings suggest that depletion of the tumor stroma through genetic ablation or pharmacologic inhibition of Sonic hedgehog (Hh) leads to a substantial increase in tumor vascularity and enhanced drug delivery in KPC mice.⁷ In human PDAC tumors, gemcitabine delivery is impeded due to increased stromal density.³⁰ Thus, we initially hypothesized that enhanced microvessel density was the result of stromal depletion and alleviation of solid stress, given the well-described role of the stroma in PDAC tumor promotion and progression.^{31–33} Using MALDI-MS we show that the combined treatment with AZD1480 and gemcitabine significantly enhances delivery of both drugs to the tumor. Interestingly however, we found that this enhanced drug delivery was not due to depletion of tumor stromal collagen or hyaluronan content. This finding was consistently seen when assessing

stromal density with both MT-MRI and second harmonic generation imaging. While preclinical studies in KPC mice have linked enhanced delivery of gemcitabine to tumor stromal depletion with Hh inhibition,⁶ we demonstrate that enhanced drug delivery is not necessarily dependent on depletion of the tumor stroma.

The failure to deplete stromal bulk may actually be a key factor in the improved therapeutic efficacy of the combination therapy. Özdemir, et al. found that depletion of myofibroblasts in the PKT mouse model led to reduced OS and an increase in immunosuppressive T-regulatory cells in the TME.⁸ Rhim, et al. also found that depletion of stromal cells with Hh inhibition resulted in formation of more aggressive and undifferentiated tumors and decreased OS.⁷ These studies clearly demonstrate that myofibroblasts and desmoplasia also play a key role in restraining PDAC, and that depletion of the stroma may be an undesirable outcome. Analysis of the stromal organization in PKT mice revealed that STAT3 inhibition combined with gemcitabine resulted in significantly increased disorganization and remodeling of the stromal collagen architecture despite retaining its bulk. The high interstitial pressure in PDAC tumors may result most directly from solid stress induced by the solid components of the tumor stroma, such as collagen and hyaluronan, and thus stromal remodeling may allow for alleviation of this solid stress without incurring the negative impact of stromal depletion.³⁴

Another key mechanism of PDAC tumor resistance to gemcitabine is through expression of Cda, which metabolizes gemcitabine leading to decreased intra-tumor levels of the drug.²⁵ Frese, et al. found that the synergistic effect of protein-bound paclitaxel is due to reduction of Cda levels through reactive oxygen species-mediated degradation and increased stabilization of gemcitabine. Our results demonstrate that STAT3 inhibition, pharmacologic or sh-RNA knockdown, significantly downregulates expression of Cda. This represents a novel finding of STAT3 inhibition that has not been previously described. Therefore, AZD1480 mediated stromal remodeling as well as downregulation of Cda in the tumor both play critical roles in the enhanced delivery of gemcitabine to the tumor as well as enhanced activity of gemcitabine within the tumor, although the relative contribution of each is yet to be determined.

Collectively, our results demonstrate that elevated STAT3 expression correlates with poor prognosis in patients with PDAC. Combining STAT3 inhibition with gemcitabine results in enhanced drug delivery of both agents and improved OS in an aggressive GEM of PDAC. The mechanism of this synergistic response is not mediated by stromal depletion, but rather through stromal remodeling and downregulation of Cda. These findings indicate that combining pharmacologic blockade of JAK/STAT3 signaling with cytotoxic gemcitabine may be an effective therapeutic strategy for patients with PDAC.

Materials and Methods

Mice

Female athymic nude mice – Foxn1 *nu/nu* (4–5 weeks old) – were purchased from Harlan Sprague Dawley, Inc. *Ptfla^{cre/+};Tgfbr2^{flox/flox}* and *LSL-Kras^{G12D/+};Tgfbr2^{flox/flox}* mice were provided by Dr. Hal Moses (Vanderbilt University Medical Center, Nashville,

Tennessee, USA). These 2 lines were intercrossed to generate *Ptf1a^{cre/+};LSL-Kras^{G12D/+};Tgfbr2^{flox/flox}* mice (PKT) on a C57Bl/6 background. Genotyping of alleles was performed using oligonucleotide primers as described previously.^{35–37}

TMA of Pancreatic Tissues

A TMA was constructed as previously described.³⁸ Eight normal pancreas, 7 chronic pancreatitis, 11 well-differentiated PDAC, 24 moderately-differentiated PDAC, and 11 poorly-differentiated PDAC tissue cores were used. TMA slides were concurrently evaluated by 2 of the authors (C.S. and N.B.M.). Nuclear and cytoplasmic staining was scored as follows: the staining index was considered as the sum of the intensity score (0, no staining; 1+, weak; 2+, moderate; 3+, strong) and the distribution score (0 – no staining; 1+ – staining of <33% of cells; 2+ – between 33% and 66% of cells; and 3+ – staining of >66% of cells). Staining indices were classified as follows: 3+ or higher – strong staining; 1+ to 2+ – weak staining; and 0 – negative staining. STAT3 and pSTAT3 were scored as positive if any detectable nuclear or cytoplasmic staining was present. For survival analysis, low pSTAT3 staining was defined as a staining index of 0 to 2+. High pSTAT3 staining was defined as an intensity score of 3+.

Treatment of PKT Mice

PKT mice were treated with vehicle, gemcitabine, AZD1480, or a combination of gemcitabine and AZD1480. Mice received twice-weekly IP injections of vehicle or 20 mg/kg of gemcitabine, starting at 4 weeks of age. Mice in the AZD1480 arm received 30 mg/kg/day by oral gavage 5 days/week, starting at 3 weeks of age. Mice were euthanized and dissected after 3 weeks unless they were part of the survival arm. Due to the irregularity of the tumor dimensions, size was determined by weighing the entire tumor. Tumor tissue was processed for further immunohistochemical and second harmonic generation examination. Overall survival was determined by log-rank analysis using Stata (version 13.1).

Second Harmonic Generation Imaging

Collagen second harmonic generation (SHG) imaging was performed on a custom built multi-photon microscope (Prairie Technologies), as described previously.³⁹ Briefly, excitation and emission light were coupled through a 40× oil immersion objective (1.3 NA) within an inverted microscope (Nikon, TiE). A titanium:sapphire laser (Coherent) was tuned to 900 nm (average power 8.4–8.6 mW) for SHG imaging. A dichroic mirror, 500nm, and a bandpass filter, 450/35 nm, isolated SHG emission light. A pixel dwell time of 4.8 microseconds was used to acquire 1024×1024 pixel images. Each image was frame averaged 8 times to reduce noise. Collagen alignment was quantified from the SHG images using the curvelet-based alignment analysis software, CurveAlign (<http://loci.wisc.edu/software/curvealign>). Collagen density was quantified by Hessian filter vessel segmentation.

Statistical Analysis

Descriptive statistics were calculated using Microsoft Excel and Prism software (Graphpad). Results are shown as values of mean ± s.d. unless otherwise indicated. Statistical analyses of

immunohistochemistry data were performed using the ANOVA followed by Tukey's multiple comparisons test to determine *P*-values. The 2-sided Student's *t* test was used for statistical analysis, with $P < 0.05$ taken as significant, except when indicated otherwise. Kaplan-Meier survival analysis was performed, and survival differences between groups were assessed with the log-rank test.

Study Approval

All animal experimental protocols were approved by the IACUC of Vanderbilt University and conducted according to the Association for the Assessment and Accreditation of Laboratory Animal Care guidelines.

The reader is referred to the Supplementary Materials and Methods section for cell lines, immunohistochemistry, Western blot analysis, xenograft models, MALDI-MS, MRI, *in vivo* bioluminescence imaging, STAT3 gene knockdown by shRNA and orthotopic injections.

Supplementary Material

Refer to Web version on PubMed Central for supplementary material.

Acknowledgements

We thank Mr. Frank Revetta and Ms. Yanhua Xiong for their technical assistance, Dr. Daniel Colvin for his technical assistance with MT-MRI acquisition, Dr. Pengcheng Lu for his assistance with statistical analysis, and Dr. Joseph Roland from the Epithelial Biology Core for his assistance with histologic analysis.

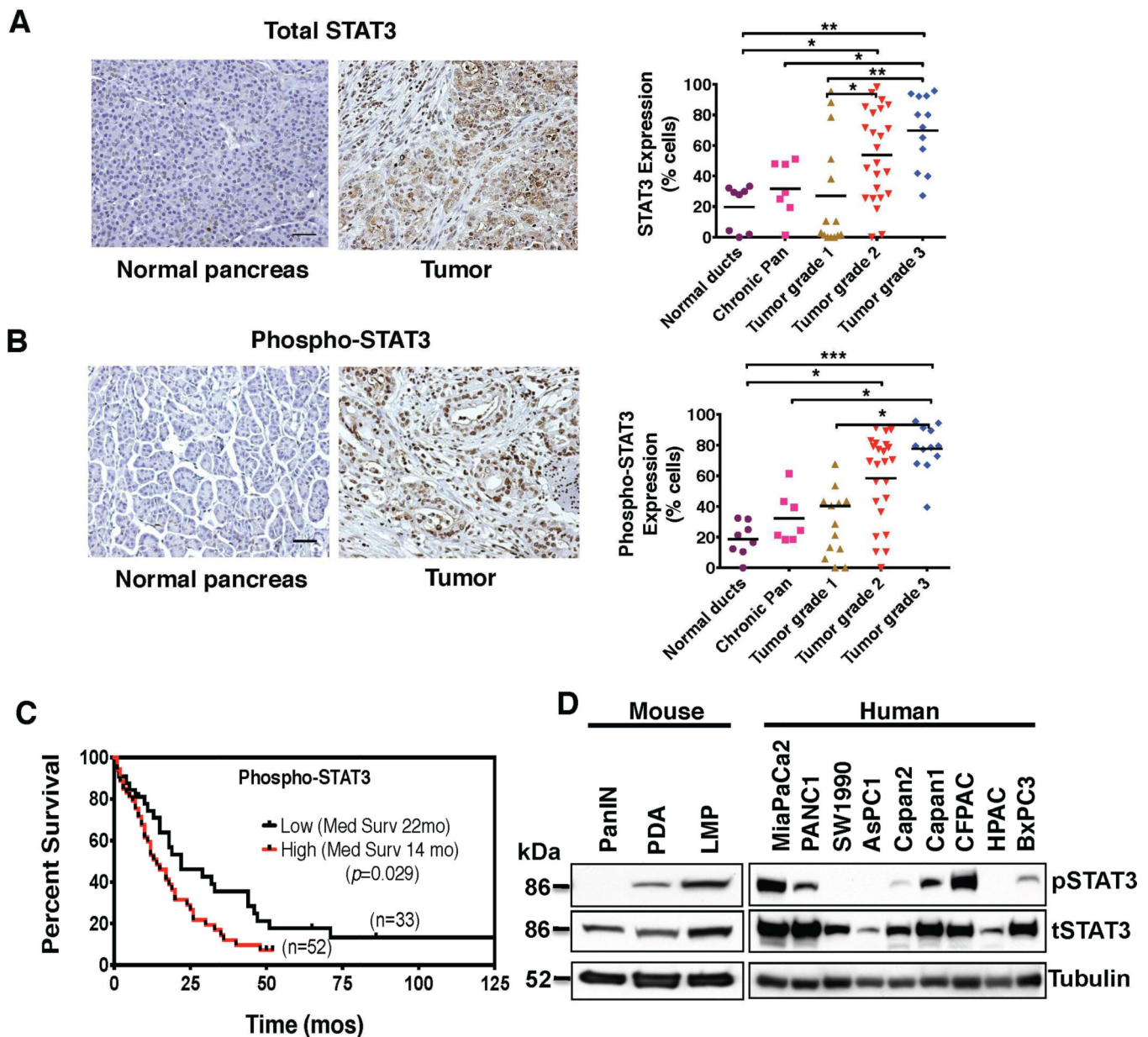
Financial Support: This work was supported by the NIH Grants CA161976, P50 95103 GI Special Program of Research Excellence Grant (SPORE), 5P30DK058404-08 Vanderbilt Digestive Disease Research Center (DDRC) Translational Award and NCI Cancer Center Support Grant #P30 CA068485-1 to N. B. Merchant. NSF Graduate Research Fellowship DGE-0909667 to A.J. Walsh. NIH Grant T32 CA 106183-10 to J. A. Castellanos. NIH Grant NCI R01 CA185747 to M. C. Skala. Core services were performed through the NIH DDRC P30DK058404 grant (N.B. Merchant and N.S. Nagathihalli).

References

1. Jemal A, Siegel R, Ward E, et al. Cancer statistics, 2008. *CA Cancer J Clin.* 2008; 58:71–96. [PubMed: 18287387]
2. Olson P, Chu GC, Perry SR, et al. Imaging guided trials of the angiogenesis inhibitor sunitinib in mouse models predict efficacy in pancreatic neuroendocrine but not ductal carcinoma. *Proc Natl Acad Sci U S A.* 2011; 108:E1275–E1284. [PubMed: 22084065]
3. Komar G, Kauhanen S, Liukko K, et al. Decreased blood flow with increased metabolic activity: a novel sign of pancreatic tumor aggressiveness. *Clin Cancer Res.* 2009; 15:5511–5517. [PubMed: 19706808]
4. Algül H, Treiber M, Lesina M, et al. Mechanisms of disease: chronic inflammation and cancer in the pancreas--a potential role for pancreatic stellate cells? *Nat Clin Pract Gastroenterol Hepatol.* 2007; 4:454–462. [PubMed: 17667994]
5. Maity A, Bernhard EJ. Modulating tumor vasculature through signaling inhibition to improve cytotoxic therapy. *Cancer Res.* 2010; 70:2141–2145. [PubMed: 20179191]
6. Olive KP, Jacobetz MA, Davidson CJ, Gopinathan A, et al. Inhibition of Hedgehog signaling enhances delivery of chemotherapy in a mouse model of pancreatic cancer. *Science.* 2009; 324:1457–1461. [PubMed: 19460966]
7. Rhim AD, Oberstein PE, Thomas DH, et al. Stromal Elements Act to Restrain, Rather Than Support, Pancreatic Ductal Adenocarcinoma. *Cancer Cell.* 2014; 25:735–747. [PubMed: 24856585]

8. Ozdemir BC, Pentcheva-Hoang T, Carstens JL, et al. Depletion of Carcinoma-Associated Fibroblasts and Fibrosis Induces Immunosuppression and Accelerates Pancreas Cancer with Reduced Survival. *Cancer Cell*. 2014; 25:719–734. [PubMed: 24856586]
9. Mace TA, Bloomston M, Lesinski GB. Pancreatic cancer-associated stellate cells: A viable target for reducing immunosuppression in the tumor microenvironment. *Oncoimmunology*. 2013; 2:e24891. [PubMed: 24073373]
10. Nagaraj NS, Washington MK, Merchant NB. Combined blockade of Src kinase and epidermal growth factor receptor with gemcitabine overcomes STAT3-mediated resistance of inhibition of pancreatic tumor growth. *Clin Cancer Res*. 2011; 17:483–493. [PubMed: 21266529]
11. Herreros-Villanueva M, Hijona E, Cosme A, et al. Mouse models of pancreatic cancer. *World J Gastroenterol*. 2012; 18:1286–1294. [PubMed: 22493542]
12. Ijichi H, Chytil A, Gorska AE, et al. Aggressive pancreatic ductal adenocarcinoma in mice caused by pancreas-specific blockade of transforming growth factor-beta signaling in cooperation with active Kras expression. *Genes Dev*. 2006; 20:3147–3160. [PubMed: 17114585]
13. Wagner M, Kleeff J, Friess H, et al. Enhanced expression of the type II transforming growth factor-beta receptor is associated with decreased survival in human pancreatic cancer. *Pancreas*. 1999; 19:370–376. [PubMed: 10547197]
14. Venkatasubbarao K, Ahmed MM, Mohiuddin M, et al. Differential expression of transforming growth factor beta receptors in human pancreatic adenocarcinoma. *Anticancer Res*. 2000; 20:43–51. [PubMed: 10769633]
15. Miyabayashi K, Ijichi H, Mohri D, et al. Erlotinib prolongs survival in pancreatic cancer by blocking gemcitabine-induced MAPK signals. *Cancer Res*. 2013; 73:2221–2234. [PubMed: 23378339]
16. Hingorani SR, Petricoin EF, Maitra A, et al. Preinvasive and invasive ductal pancreatic cancer and its early detection in the mouse. *Cancer Cell*. 2003; 4:437–450. [PubMed: 14706336]
17. Hingorani SR, Wang L, Multani AS, et al. Trp53R172H and KrasG12D cooperate to promote chromosomal instability and widely metastatic pancreatic ductal adenocarcinoma in mice. *Cancer Cell*. 2005; 7:469–483. [PubMed: 15894267]
18. Nagaraj NS, Smith JJ, Revetta F, et al. Targeted inhibition of SRC kinase signaling attenuates pancreatic tumorigenesis. *Mol Cancer Ther*. 2010; 9:2322–2332. [PubMed: 20682659]
19. Schust J, Sperl B, Hollis A, et al. Stattic: a small-molecule inhibitor of STAT3 activation and dimerization. *Chem Biol*. 2006; 13:1235–1242. [PubMed: 17114005]
20. Reyzer ML, Caldwell RL, Dugger TC, et al. Early changes in protein expression detected by mass spectrometry predict tumor response to molecular therapeutics. *Cancer Res*. 2004; 64:9093–9100. [PubMed: 15604278]
21. Reyzer ML, Caprioli RM. MALDI-MS-based imaging of small molecules and proteins in tissues. *Curr Opin Chem Biol*. 2007; 11:29–35. [PubMed: 17185024]
22. Provenzano PP, Cuevas C, Chang AE, et al. Enzymatic targeting of the stroma ablates physical barriers to treatment of pancreatic ductal adenocarcinoma. *Cancer Cell*. 2012; 21:418–429. [PubMed: 22439937]
23. Li W, Zhang Z, Nicolai J, et al. Magnetization transfer MRI in pancreatic cancer xenograft models. *Magn Reson Med*. 2012; 68:1291–1297. [PubMed: 22213176]
24. Cicchi R, Kapsokalyvas D, De Giorgi V, et al. Scoring of collagen organization in healthy and diseased human dermis by multiphoton microscopy. *J Biophotonics*. 2010; 3:34–43. [PubMed: 19771581]
25. Frese KK, Neesse A, Cook N, et al. nab-Paclitaxel potentiates gemcitabine activity by reducing cytidine deaminase levels in a mouse model of pancreatic cancer. *Cancer discovery*. 2012; 2:260–269. [PubMed: 22585996]
26. Liu L, McBride KM, Reich NC. STAT3 nuclear import is independent of tyrosine phosphorylation and mediated by importin-alpha3. *Proc Natl Acad Sci U S A*. 2005; 102:8150–8155. [PubMed: 15919823]
27. Yang J, Liao X, Agarwal MK, et al. Unphosphorylated STAT3 accumulates in response to IL-6 and activates transcription by binding to NFkappaB. *Genes Dev*. 2007; 21:1396–1408. [PubMed: 17510282]

28. Lesina M, Kurkowski MU, Ludes K, et al. Stat3/Socs3 activation by IL-6 transsignaling promotes progression of pancreatic intraepithelial neoplasia and development of pancreatic cancer. *Cancer Cell*. 2011; 19:456–469. [PubMed: 21481788]
29. Carmeliet P, Jain RK. Principles and mechanisms of vessel normalization for cancer and other angiogenic diseases. *Nat Rev Drug Discov*. 2011; 10:417–427. [PubMed: 21629292]
30. Koay EJ, Truty MJ, Cristini V, et al. Transport properties of pancreatic cancer describe gemcitabine delivery and response. *J Clin Invest*. 2014; 124:1525–1536. [PubMed: 24614108]
31. Ikenaga N, Ohuchida K, Mizumoto K, et al. CD10+ pancreatic stellate cells enhance the progression of pancreatic cancer. *Gastroenterology*. 2010; 139:1041–1051. 1051 e1–1051 e8. [PubMed: 20685603]
32. Lonardo E, Frias-Aldeguer J, Hermann PC, et al. Pancreatic stellate cells form a niche for cancer stem cells and promote their self-renewal and invasiveness. *Cell Cycle*. 2012; 11:1282–1290. [PubMed: 22421149]
33. Xu Z, Vonlaufen A, Phillips PA, et al. Role of pancreatic stellate cells in pancreatic cancer metastasis. *Am J Pathol*. 2010; 177:2585–2596. [PubMed: 20934972]
34. Chauhan VP, Boucher Y, Ferrone CR, et al. Compression of pancreatic tumor blood vessels by hyaluronan is caused by solid stress and not interstitial fluid pressure. *Cancer Cell*. 2014; 26:14–15. [PubMed: 25026209]
35. Chytil A, Magnuson MA, Wright CV, et al. Conditional inactivation of the TGF-beta type II receptor using Cre:Lox. *Genesis*. 2002; 32:73–75. [PubMed: 11857781]
36. Kawaguchi Y, Cooper B, Gannon M, et al. The role of the transcriptional regulator Ptf1a in converting intestinal to pancreatic progenitors. *Nat Genet*. 2002; 32:128–134. [PubMed: 12185368]
37. Jackson EL, Willis N, Mercer K, et al. Analysis of lung tumor initiation and progression using conditional expression of oncogenic K-ras. *Genes Dev*. 2001; 15:3243–3248. [PubMed: 11751630]
38. Cates JM, Byrd RH, Fohn LE, et al. Epithelial-mesenchymal transition markers in pancreatic ductal adenocarcinoma. *Pancreas*. 2009; 38:e1–e6. [PubMed: 18766116]
39. Walsh AJ, Cook RS, Manning HC, et al. Optical metabolic imaging identifies glycolytic levels, subtypes, and early-treatment response in breast cancer. *Cancer Res*. 2013; 73:6164–6174. [PubMed: 24130112]

**Figure 1.**

STAT3 expression is associated with chemoresistance and overall survival in PDAC patients. (A) and (B) Representative tissue sections from a TMA constructed from patient samples are shown (left panels). The tissues were grouped by diagnosis and grade, and percentage of cells positively stained for total STAT3 are shown (scale bar = 0.5 mm). (A) Total and (B) pSTAT3 expression increased in a step-wise fashion from normal pancreas to chronic pancreatitis and through advancing grades of PDAC (right panels). (C) Kaplan-Meier survival curve comparing overall survival for patients with PDAC stratified by level of pSTAT3 staining. Patients with high pSTAT3 expression have significantly decreased overall survival compared with patients with low pSTAT3 expression. (D) Expression of pSTAT3 and total STAT3 in pancreatic cell lines generated from PanIN, primary PDAC (PDA) and

liver metastatic (LMP) lesions from KC (PanIN) and KPC (PDA and LMP) mice (left panel), and in human PDAC cell lines (right panel) are demonstrated. Abbreviations: tSTAT3 – total-STAT3; pSTAT3 – phospho-STAT3; * – $P < 0.05$; ** – $P < 0.01$; *** – $P < 0.001$.

Author Manuscript

Author Manuscript

Author Manuscript

Author Manuscript

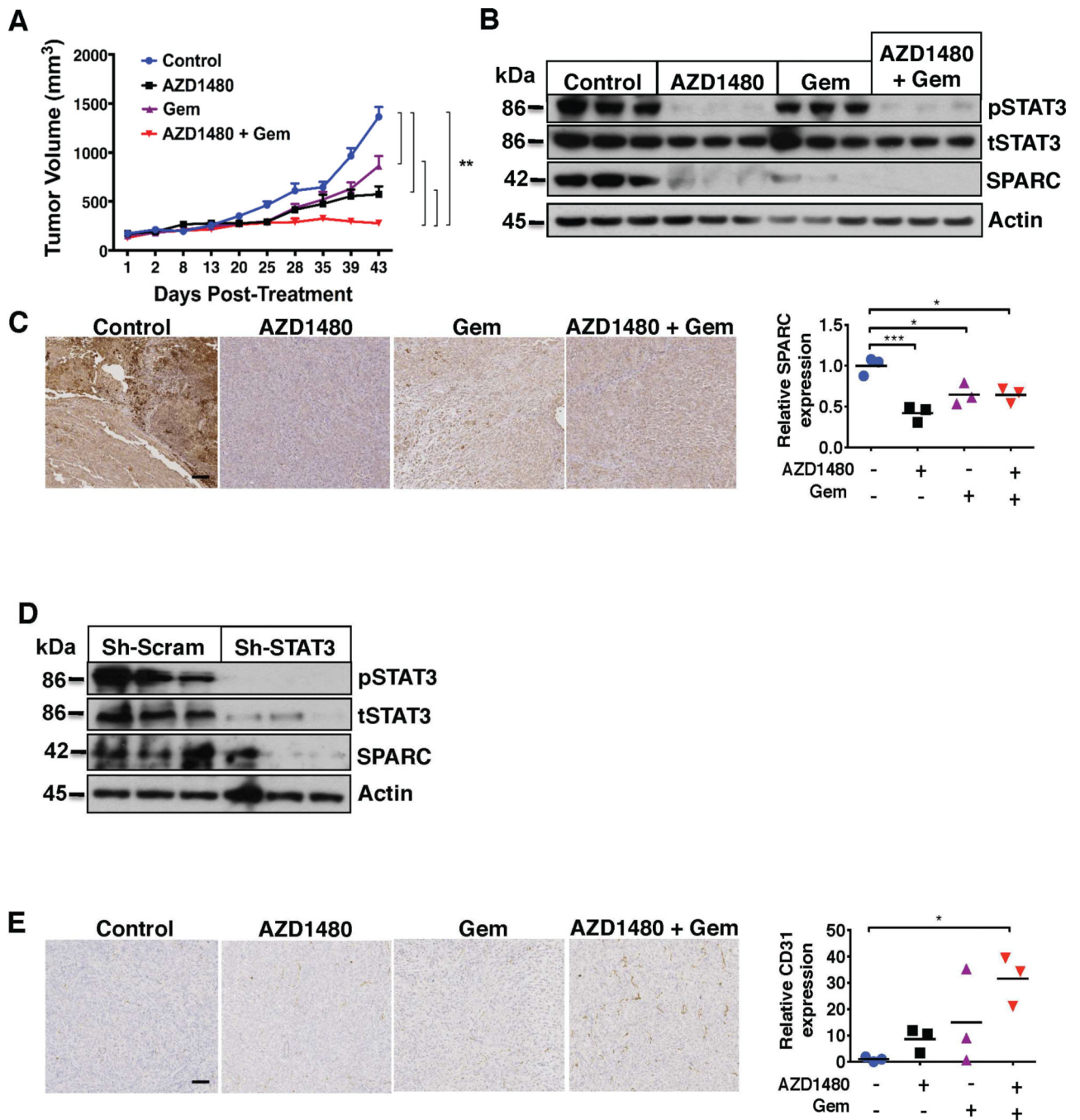


Figure 2. Combined AZD1480 and gemcitabine treatment decreases tumor growth and alters the tumor microenvironment in PDAC xenograft models. (A) AZD1480 with gemcitabine (Gem) induces *in vivo* tumor regression. Growth rate of PANC1 flank xenografts in Fox1-*nu/nu* mice treated with vehicle, AZD1480, Gem, or AZD1480/Gem treatment. Error bars indicate SD of mean; n = 5 per group. ** – P < 0.01. (B) Orthotopic pancreatic injections of luciferase tagged PANC1 cells were treated with vehicle, AZD1480, Gem, or AZD1480/Gem treatment. Tumor xenograft tissues (n=3) were analyzed for total STAT3,

pSTAT3 and SPARC expression by immunoblot analysis. AZD1480/Gem treatment significantly inhibits expression of pSTAT3 and SPARC. (C) Immunohistochemistry of orthotopic pancreatic tumor xenograft tissues show decreased SPARC expression with AZD1480 and AZD1480/Gem treatment. Left panels show representative examples of tumor tissues stained with SPARC (scale bar= 0.5 mm) and the quantified graph in the right panel. * – $p < 0.05$; *** – $P < 0.001$. (D) Analysis of tumor lysates of orthotopic pancreas injections of Sh-scrambled and Sh-STAT3 PANC1 cells show that Sh-STAT3 PANC1 tumors have significantly decreased expression of pSTAT3 and SPARC (E) Orthotopic pancreatic tumor xenograft tissues were stained with CD31 antibody to measure microvessel density. Left panels show representative examples of tumor tissues stained with CD31 (scale bar=0.5 mm) and the quantified graph in the right panel. CD31 staining showed markedly increased microvessel density with AZD1480/Gem combined therapy. * – $p < 0.05$.

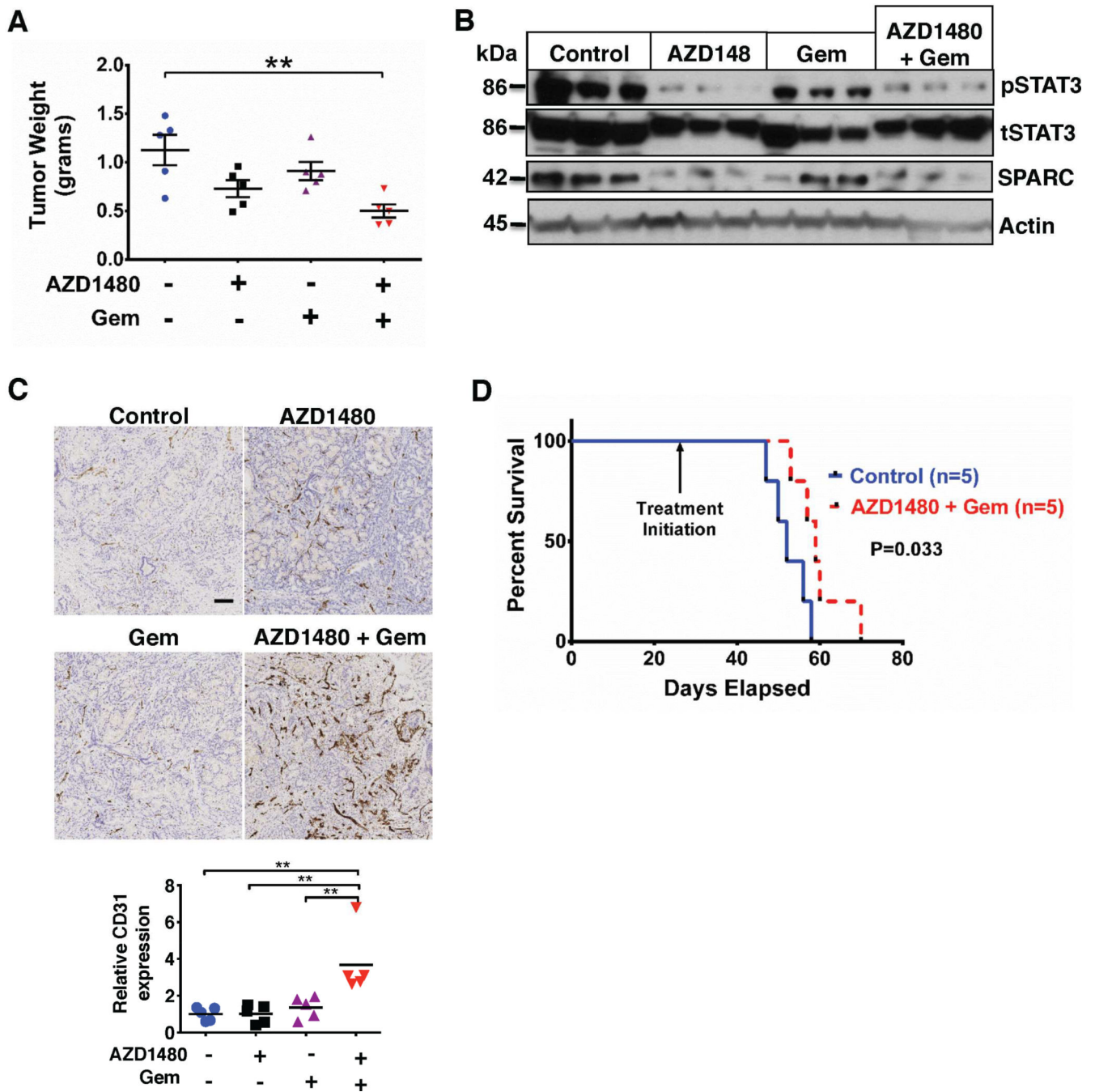


Figure 3. Combined AZD1480 and gemcitabine treatment alters the tumor microenvironment and improves survival of PKT mice. (A) PKT mice were treated with vehicle, AZD1480, Gem, or combined AZD1480/Gem. Tumor weight in the AZD1480/Gem treated mice was significantly decreased compared with vehicle treated controls. ** – P < 0.01. (B) Western blot analysis of whole tumor lysates from PKT mice demonstrated decreased expression of pSTAT3 and SPARC in mice treated with AZD1480 or AZD1480/Gem compared with vehicle control mice. (C) Microvessel density (assessed by staining for CD31) was

significantly increased with AZD1480/Gem treatment. Upper panels show representative examples of tumor tissues stained with CD31 (scale bar=0.5 mm) and the quantified graph is shown in the lower panel. ** – $P < 0.01$. (D) Kaplan-Meier survival analysis shows significantly improved overall survival with AZD1480/Gem (median 60 days) compared with vehicle control (median 52 days, log rank test, $p = 0.033$).

Author Manuscript

Author Manuscript

Author Manuscript

Author Manuscript

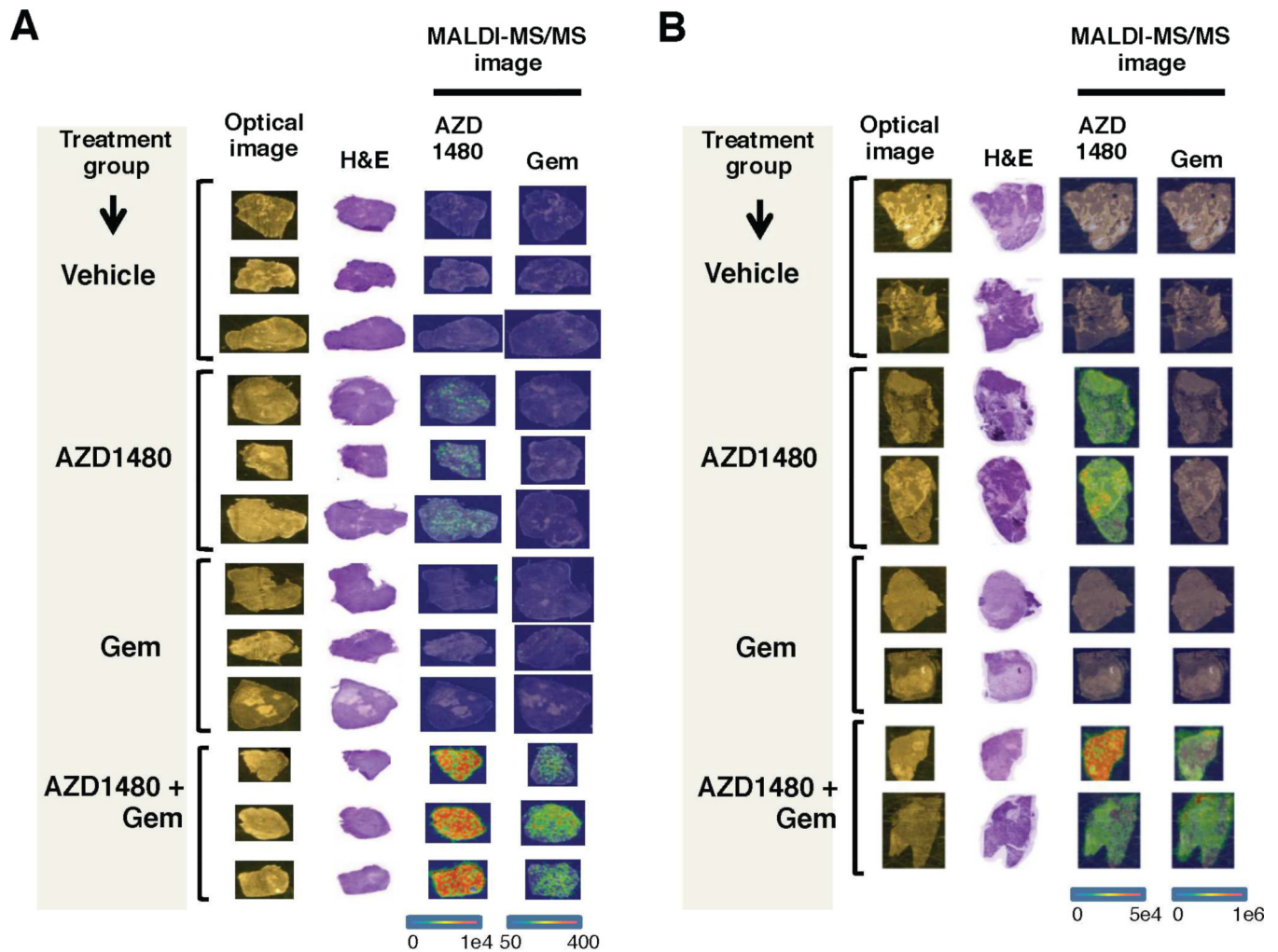


Figure 4.

AZD1480 and gemcitabine treatment enhances tumor drug delivery. MALDI-MS/MS analysis of pancreatic tumor xenograft tissues was conducted to detect the presence of AZD1480 and Gem within the tumor. The optical image column demonstrates tissues prior to matrix coating; the H&E column contains stained serial sections. The MALDI-MS/MS images are divided into two columns, the first demonstrating detection of AZD1480 (m/z 255 and 257) and the second demonstrating detection of Gem (m/z 112). (A) MS images of the localization of AZD1480 and Gem in subcutaneous xenograft tissue sections. (B) MS images of the localization of AZD1480 and Gem in orthotopic xenograft tissue sections. The combination of AZD1480 and Gem results in enhanced *in vivo* delivery of both drugs in pancreatic tumor xenografts. The color scale ranges from blue to red, with red representing high concentration and blue representing low concentration of drug detected.

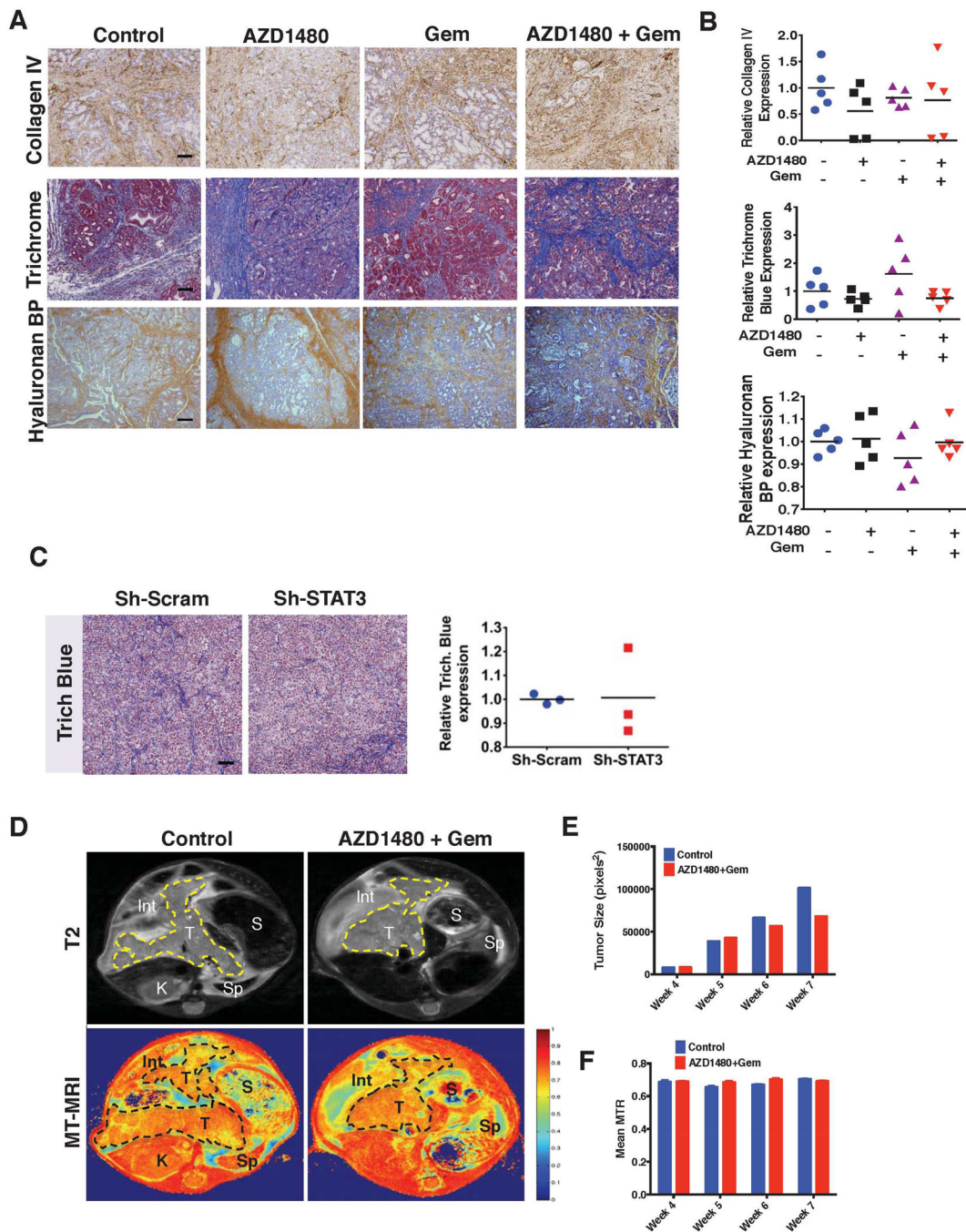


Figure 5. AZD1480 and gemcitabine treatment does not alter stromal density. (A) Tumors from PKT mice treated with vehicle, AZD1480, Gem, or AZD1480/Gem were stained for collagen IV, trichrome Blue, and hyaluronan binding protein (BP) (Scale bars=0.5 mm). (B) Quantitative analysis of collagen IV, trichrome blue, and hyaluronan BP revealed no significant difference in collagen or hyaluronan density after any treatment. (C) Stromal effects of STAT3 knock down (Sh-STAT3). Sh-Scram and Sh-STAT3 PANC1 cells were injected into the flanks of Fox1-*nu/nu* mice and harvested when mice were euthanized. Trichrome blue

stain was performed and collagen density was calculated by quantifying collagen staining and shows no difference between the two groups. (*D*) Magnetization Transfer (MT)-MRI was utilized to follow the longitudinal effects of combined AZD1480/Gem treatment on stromal fibrosis. Representative T2-MRI and MT-MRI images of 7-week-old PKT mice are shown. A region of interest (ROI) circumscribing the pancreas was determined for each axial slice, and tumor size (*E*) and mean magnetization transfer ratio (MTR) (*F*) were calculated at each time point. ROI's (yellow dashed line in T2 axial images, top panels, and a black dashed line MT axial images, bottom panels) show a clear decrease in tumor volume with AZD1480/Gem treatment, but no effect on MTR. Int – intestine; K – kidney; S – stomach; Sp – spleen; T – tumor.

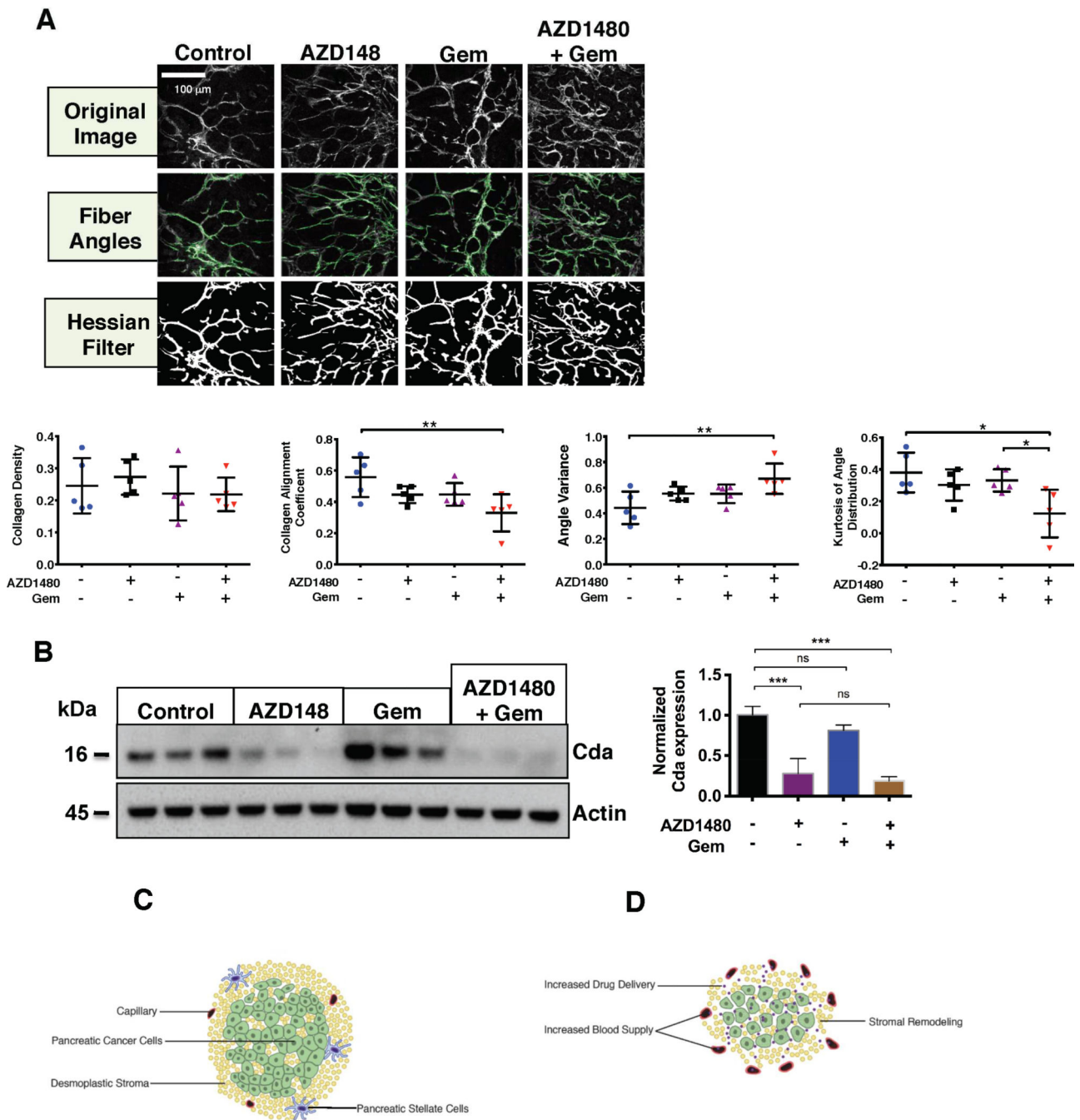


Figure 6. AZD1480 and gemcitabine treatment remodels the tumor stroma. (A) Collagen second harmonic generation (SHG) imaging was performed on tumor tissue collected from PKT mice treated with vehicle, AZD1480, Gem, or AZD1480/Gem. Upper panels show representative images from each treatment group for fiber angles and hessian filter. In the lower panels, graphs show significantly increased angle variance and significantly decreased collagen alignment coefficient and kurtosis of angle distribution with AZD1480/Gem treatment. Collagen density was unchanged between treatment groups. * – P < 0.05; ** – P

< 0.01. (B) Tumor lysates from PKT mice were analyzed for Cytidine deaminase (Cda) expression revealing significantly decreased expression of Cda with AZD1480 or AZD1480/Gem treatment (left panel). Quantitative analysis by densitometry of Cda expression is shown on the right. ns – non significant ; *** – $P < 0.001$. (C) PDAC is characterized by dense stroma and poor vascularity. PSCs secrete IL-6, leading to STAT3 activation and enhanced tumorigenicity in PDAC cells. (D) Combined STAT3 inhibition and gemcitabine treatment results in enhanced drug delivery, increased microvessel density, and stromal remodeling.